Journal of Vacuum Science and Technology B

RESEARCH ARTICLE | JUNE 08 2023

Rapid detection of radiation susceptible regions in electronics

Sergei P. Stepanoff ; Aman Haque ; Fan Ren ; Stephen Pearton ; Douglas E. Wolfe

J. Vac. Sci. Technol. B 41, 044005 (2023)
https://doi.org/10.1116/6.0002689

07 April 2024 11:13:51

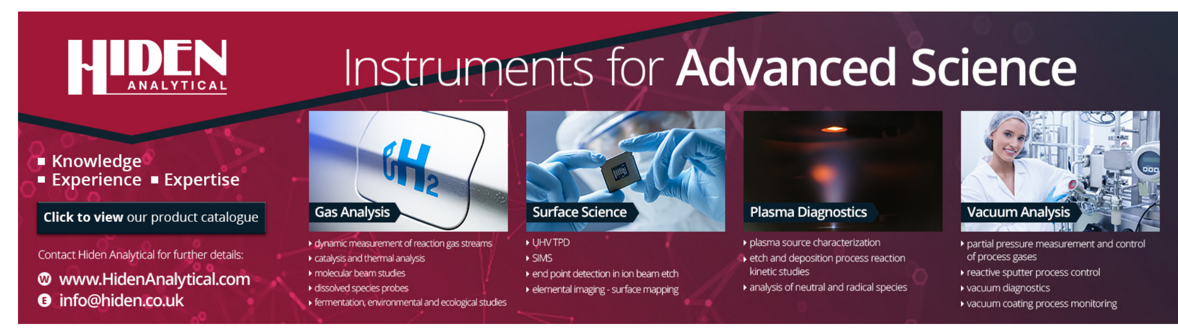

JVST B
Journal of Vacuum Science & Technology B

ARTICLE

avs.scitation.org/journal/jvb

Rapid detection of radiation susceptible regions in electronics

Cite as: J. Vac. Sci. Technol. B **41**, 044005 (2023); doi: 10.1116/6.0002689
Submitted: 18 March 2023 · Accepted: 8 May 2023 ·
Published Online: 8 June 2023

View Online

Export Citation

CrossMark

Sergei P. Stepanoff,[1,2] Aman Haque,[3,a)] Fan Ren,[4] Stephen Pearton,[5] and Douglas E. Wolfe[1,2,6,7,b)]

AFFILIATIONS

[1]Materials Science and Engineering Department, The Pennsylvania State University, University Park, Pennsylvania 16802
[2]Applied Research Laboratory, The Pennsylvania State University, University Park, Pennsylvania 16802
[3]Mechanical Engineering, The Pennsylvania State University, University Park, Pennsylvania 16802
[4]Chemical Engineering, University of Florida, Gainesville, Florida 32611
[5]Material Science and Engineering, University of Florida, Gainesville, Florida 32611
[6]Engineering Science and Mechanics Department, The Pennsylvania State University, University Park, Pennsylvania 16802
[7]Ken and Mary Alice Lindquist Nuclear Engineering Department, The Pennsylvania State University, University Park, Pennsylvania 16802

[a)]**Author to whom correspondence should be addressed:** mah37@psu.edu
[b)]**Electronic mail:** dew125@arl.psu.edu

07 April 2024 11:13:51

ABSTRACT

Radiation susceptibility of electronics has always been about probing electrical properties in either transient or time-accumulated phenomena. As the size and complexity of electronic chips or systems increase, detection of the most vulnerable regions becomes more time consuming and challenging. In this study, we hypothesize that localized mechanical stress, if overlapping electrically sensitive regions, can make electronic devices more susceptible to radiation. Accordingly, we develop an indirect technique to map mechanical and electrical hotspots to identify radiation-susceptible regions of the operational amplifier AD844 to ionizing radiation. Mechanical susceptibility is measured using pulsed thermal phase analysis via lock-in thermography and electrical biasing is used to identify electrically relevant regions. A composite score of electrical and mechanical sensitivity was constructed to serve as a metric for ionizing radiation susceptibility. Experimental results, compared against the literature, indicate effectiveness of the new technique in the rapid detection of radiation-vulnerable regions. The findings could be attractive for larger systems, for which traditional analysis would take —two to three orders of magnitude more time to complete. However, the indirect nature of the technique makes the study more approximate and in need for more consistency and validation efforts.

Published under an exclusive license by the AVS. https://doi.org/10.1116/6.0002689

I. INTRODUCTION

Modern electronic systems employ increasingly complex designs that must continue functioning when exposed to ionizing radiation, as in space, aviation, defense, medicine, and nuclear power applications. As a result, electronics that are not sensitive to ionizing radiation or “rad hard” electronics are desirable for applications with radiation environments. Inevitably, some regions and transistors within integrated electronics are more susceptible to certain types of ionizing radiation interactions, such as single event effects (SEEs) and total ionizing dose (TID) effects. For SEEs, a single incoming particle causes a cascade of ionization within the semiconducting material of electronics, creating transients that can produce device faults.[1–5] TID effects can produce charge traps in oxide layers that are present in bipolar junction transistors (BJTs) and field effect transistors (FETs) due to the net positive charge they leave at the oxide interfaces.[6,7] In order to effectively design rad hard electronics, the most sensitive components need to be identified so that they can be selectively hardened. Identification of the most vulnerable regions (MVRs) in electronics is difficult since the amount of charge generated from ionizing radiation, their

Published under an exclusive license by the AVS

diffusion toward charge collectors, and the tendency to get trapped in the semiconductor or the interfaces are not uniform over the electronic devices or systems. These parameters vary spatially due to materials, interfaces, geometry, operation, and fabrication conditions. Thus, for a large system on a chip, pinpointing MVRs based on the global circuit response to ionizing radiation can be extremely time consuming. In order to gain significant insight into the behavior of different electronic system components, specialized techniques have been and are currently under development, the most advanced of which uses a pulsed laser to cause localized ionization in semiconductor electronics, after which a transient current response is measured from the circuitry.[8–14] Other techniques include *in situ* software-based diagnosis of components that experience upsets, often using a microbeam of radiation or radiation surrogate to improve the identification of MVRs.[15]

State-of-the-art methods for MVR identification are time consuming and generally limited to inspection of small, manageable regions. For example, an entire $50 \times 50\,\text{mm}^2$ integrated circuit would take on the order of months or years to measure with a pulsed-laser technique, which is compounded by the increasing complexity of modern electronic systems. Ideally, an experimental protocol that would be able to quickly detect the most vulnerable regions in an electronic system would provide a disruptive improvement to the efficiency of selective hardening of electronics. Such a protocol would be able to complement current state-of-the-art techniques by narrowing down the potential regions of susceptibility and providing a short-list of regions to interrogate, using currently validated techniques. For example, identification of the most susceptible $100 \times 100\,\mu\text{m}^2$ regions on a $50 \times 50\,\text{mm}^2$ chip can reduce the conventional effort by a time scale of up to 2 50 000 times.

The objective of this study is to demonstrate feasibility of a rapid MVR identification technique. We observe that the current literature focuses only on "electrically sensitive" regions [Fig. 1(a) in relation to SEE] to identify radiation susceptibility. We argue that while radiation vulnerability manifests through electrical characteristics (such as transient spikes in current or voltage), the root cause analysis should be broader and include localization of mechanical and thermal domains as well. Our hypothesis is that highly localized and high-magnitude mechanical stress regions may significantly alter ionization-induced charge generation and distribution. This is because the atoms in these regions have higher strain energy compared to atoms with equilibrium distance. They are also more unstable in the potential energy well and, thus, need less external energy to be displaced or to be ionized depending on the type of incoming radiation.[16,17] If such stress localization coincides with the electrically sensitive areas (such as proximity to the gate region), it can influence the overall radiation vulnerability. A corollary of this hypothesis is that for the same ionizing potential and device design, a region with higher mechanical stress localization would also imply higher radiation vulnerability. Therefore, we propose that mapping mechanical stress localization can lead to insights that are not obtained by electrical measurements alone. It is important to note that stress localization is the key, and not uniform stress field, which has been thoroughly investigated through strain engineering in devices. We observe that imperfect and heterogeneous material systems and processing conditions lead to complex three-dimensional stress states with high localized stresses along the edges of device features. Gates, vias, and materials interfaces are examples where stress concentrations are locally quite high, while attenuating quickly into the bulk features. Interestingly,

07 April 2024 11:13:51

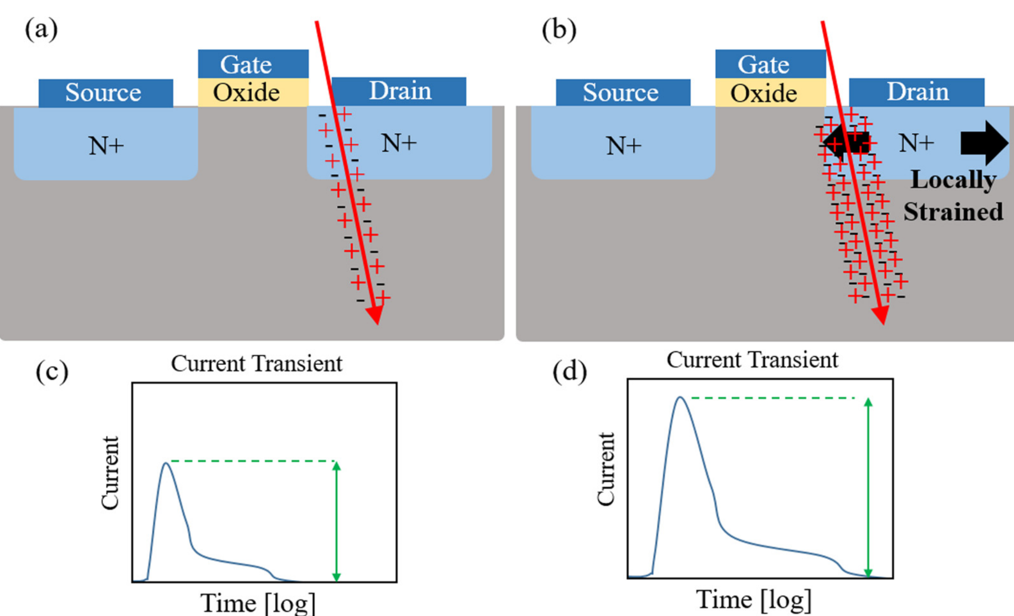

FIG. 1. Schematic of charge carrier generation following interaction of an energetic particle with (a) an unstrained and (b) a strained FET, where traps are filled with negative charge carriers at the silicon–oxide interface. Current transient profiles for the (c) unstrained and (d) strained FET.

Published under an exclusive license by the AVS

their global average value may be insignificant, but localized values can reach on the order of a few gigapascals, which can require less energy for a material to strip electrons from its bounded arrangement compared to unstressed materials. Higher concentrations of charge carriers form in strained materials for each single event as a result, causing more severe current releases into the circuitry.

The core hypothesis for this study is schematically shown in Fig. 1 for two devices electrically similar, but one with a mechanical hotspot in the gate/drain region. For the exact same energetics of incoming ionizing radiation, we expect a higher density of charges in a mechanical hotspot. Charge carriers generated from the path of ionization are often collected by local conductive regions, such as a source, drain, or gate. It is important to note that the majority of SEEs occur only if the event occurs near an electrically relevant part of the circuit, where there is a conductive node for charges to collect and deposit into nearby regions in the circuit. Therefore, regions of high electric field, where a critical charge can build up and disrupt the electrical state of the system are most relevant when identifying the most vulnerable regions in microelectronics.[18] In addition to mechanical stress concentrations (mechanical hotspots) near the gate/drain edges, electrically active regions (electrical hotspots) collectively point to a region that can be predictively identified as an MVR. Investigating both stress and electric field localization in microelectronics can, therefore, provide a predictive method for identifying radiation sensitivity without the need for conducting time consuming irradiation, while also improving the effectiveness of pulsed-laser experiments, which has been investigated in a previous work on the operational amplifier LM124.[19] This work expands upon the previous work by providing a composite metric or "score" to simplify the identification of MVRs using mechanical and electrical hotspot analysis.

Stress and strain are inherent in manufactured electronics for several reasons, including thermal expansion and contraction in lattice-mismatched epitaxial heterostructures, intrinsic stress in deposited films, defect evolution, applied external stress, etc., and can have a significant impact on the properties and performance of nearly all types of electronic components.[20] Strain can, therefore, be used to naturally enhance the properties and performance of certain electronic components, which are essential to modern systems, such as strained silicon on insulators[21] and high-electron-mobility transistors.[22] However, when not intentionally engineered into the materials, strain can be detrimental for the performance of electronic components. Especially in the case of radiation hardness, where it has been found that strain present in a transistor structure can result in significant increases in the intensities of current transients upon exposure to ionizing radiation relative to unstrained devices. When electronics experience a sudden surge of high current and voltage in a way they were not designed to handle, they can experience operational upsets and damage resulting in decreased reliability.[23] This, of course, can have severe detrimental effects on potentially imperative equipment they make up, and methods to increase their reliability in radiation environments are of high interest for several governmental, industrial, and commercial applications.

Most techniques used to evaluate the radiation hardness of electronics present logistical challenges, including cost and time constraints. For example, techniques that involve the use of ionizing radiation to probe a sample end up irreversibly damaging the component they set out to measure, which limits the testing of a device. Techniques that utilize neutrons and gamma radiation are often difficult to organize due to the limited number of facilities that house the sources that produce these forms of radiation. Additionally, identification of localized sensitivity requires microbeam interrogation that is difficult to achieve with nearly all forms of ionizing radiation. Pulsed-laser probing is a good alternative for ionizing radiation for charge carrier injection on the submicrometer scale, where the laser is scanned across the surface of an exposed chip, and the resulting transient current pulses are measured, where the highest intensity pulses correspond with the regions that are most sensitive to ionizing radiation. However, pulsed-laser single event transient (SET) measurements take quite long to conduct due to the time it takes for data writing at each location. These constraints can be mitigated with lock-in thermography (LIT), which nondestructively injects thermal waves into the surface of the sample while the re-emitted thermal signal is captured with thermograms. Upon injecting heat waves (e.g., with a flash lamp), the heat is conducted into the sample in waves that interact with nonhomogeneous regions within the object that partially reflect the input wave. The resulting interference pattern result in changes to the surface temperature, which are collected by thermographs over time and can be analyzed via phase mapping. It is hypothesized that regions that exhibit high interference with the injected thermal signal correlate with regions that exhibit high strain in the as-manufactured integrated circuits, which is expected to cause detrimental effects on the sensitivity of highly strained regions.[23,24] Regions that are electrically relevant to allow current transients throughout the electrical system are also identified so that regions that exhibit both mechanical and electrical sensitivities are highlighted as sensitive to ionizing radiation. Since data is collected in real-time and data analysis can be conducted on publicly available software (e.g., MATLAB, Python, etc.), data collection and analysis takes on the order of minutes or hours and is not cost prohibitive, which is a great improvement over existing techniques. One limitation of the proposed technique is its spatial resolution, which is several micrometers due to the diffraction limitations of the infrared light used to measure the thermal response. However, logistical benefits of this technique allow it to be used in complement with the current state-of-the-art pulsed-laser SET techniques, where LIT can be used to identify general regions of sensitivity, and the spatially resolved laser-based technique can examine those areas, saving the analysis time.

07 April 2024 11:13:51

II. EXPERIMENT

An operational amplifier AD844 was selected for analysis as it is widely used for its low distortion, low noise, stability, and wide bandwidth. Another reason is that prior studies on MVRs in this chip allow benchmarking with the literature. Figure 2 shows an optical micrograph of a decapsulated AD844 amplifier used for testing. Literature has identified five sensitive regions via pulsed-laser single event transient testing, which are labeled 1–5 in Fig. 2 in black-boxed regions.[25,26] These regions produced single event transients with the highest voltage amplitudes and pulse widths when probed with a pulsed-laser system. Regions 1 and 2 correspond to differential inputs, region 3 is part of the –Vs circuit

Published under an exclusive license by the AVS

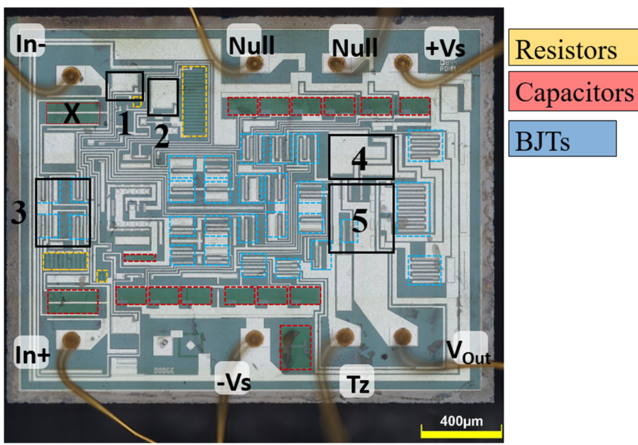

FIG. 2. Optical micrograph of the decapsulated operational amplifier AD844 with the most vulnerable regions labeled 1–5 as well as resistors, capacitors, and BJT. The scale bar is 400 μm.

element, region 4 contains the TZ circuit, which is used to obtain a high slew-rate, and region 5 is part of the output stage. Several circuit elements are labeled on the micrograph in Fig. 2, including resistors, capacitors, and bipolar junction transistors (BJTs). We are able to identify BJTs from their emitter, base collector, and structure, which are typically seen as three parallel metalized lines on the circuit. Resistors are typically identifiable from their snaking pattern, and capacitors are generally large area features. For analysis, we also selected a capacitor that we expected would not be particularly sensitive relative to the identified regions in the literature for later comparison and labeled this region with an "X."

In order to identify the MVRs, a two-part approach is utilized, where (1) LIT is used to identify the regions with the highest mechanical strain and (2) electrical biasing of the operational amplifier AD844 is used in conjunction with thermal imaging to identify the regions with the highest electric field through joule heating; these techniques are schematically shown in Figs. 3(a) and 3(b), respectively. If a region meets the conditions of having both a high mechanical and high electrical propensity for being sensitive to irradiation, the region has a higher likelihood of being identified as an MVR.

With LIT, an emissivity-corrected phase map of the AD844 amplifier is produced by injecting thermal waves at a constant lock-in frequency into it using a heat lamp, while the re-emitted thermal response is measured using a thermal camera. In order to construct the phase map from the thermal video file, the temperature response of each pixel with respect to time was multiplied by two orthogonal weighting factors [i.e., sin(t) and –cos(t)], each with a frequency that matches the lock-in frequency, and the results were summed for each pixel. After summation, each pixel has two values assigned, including (1) $S^{0°}$—the in-phase component of the re-emitted signal—and (2) $S^{-90°}$—the out-of-phase component of the re-emitted signal.[27] Using both $S^{0°}$ and $S^{90°}$ signals, the phase value for each pixel, which represents the degree of lag between the re-emitted thermal signal versus a reference signal, can be calculated using Eq. (1). The regions that exhibit the highest difference in phase contrast values correspond to the regions with the highest thermal stopping power based on the underlying structure of the device,

$$\text{Phase} = \tan^{-1}\left(\frac{S^{-90°}}{S^{0°}}\right). \quad (1)$$

The thermal camera used for both the mechanical and electrical measurements was the Optris PI 640 IR camera with a noise equivalent temperature difference of 75 mK over the spectral range of 8–14 μm. Each lock-in thermography measurement was made with 2000 frames of data, which were processed postmeasurement to calculate the phase maps. Part of this calculation included the removal of noise in the thermal data that did not modulate with the lock-in frequency, which was carried out using a bandpass filter. Up to two orders of magnitude improvement in the thermal sensitivity of LIT measurements over the thermal sensitivity of the camera was possible due to the time averaging nature of lock-in

07 April 2024 11:13:51

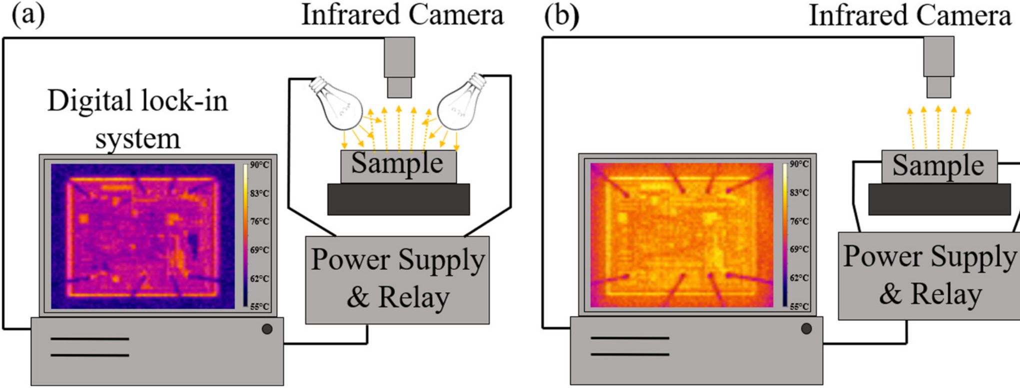

FIG. 3. Schematic of (a) the LIT setup and (b) the electrical biasing setup for electrical activity measurements.

Published under an exclusive license by the AVS

thermography. In order to heat the chips in pulses, two heat lamps were triggered using a two-channel 5 V relay module and a programmable Arduino board. Prior to each measurements, the average temperature of the AD844 amplifier was allowed to equalize by exposing the board to the pulsing heat lamps for 30 min before data were collected, which allowed a consistent temperature throughout the entirety of the measurement.

III. RESULTS AND DISCUSSION

Field measurements were conducted using a thermal camera to measure the temperature of the AD844 amplifier between the biased and unbiased conditions. The AD844 amplifier was hooked up to a power supply with ±6 V using a virtual ground circuit and was configured as a noninverting amplifier as shown in the circuit diagram in Fig. 4(c). After powering, Joule heating caused local raises in temperature on the chip as shown in Fig. 4(a) (before powering) and 4(b) (after powering). However, unlike the phase map of the lock-in thermography measurements, these thermal micrographs are still influenced by emissivity differences in the surface materials, where metalized regions appear to have a higher temperature even when we are certain all regions have the same temperature, as in Fig. 4(a). To aid in mitigating the error introduced by local emissivity differences, the differences in temperature before and after biasing were mapped and shown in Fig. 4(d), which gives an idea of the regions that are more electrically active. It is important to note that evaporating a thin coating of carbon can mitigate the emissivity concerns. This technique was not used in this study because of our future plans in performing *in situ* biasing of the device under tests (DUTs).

An important aspect of the proposed technique is the ability to interrogate different depths in the DUT since the heating frequency dictates the thermal penetration depth. It is the distance reached by the heat during a time of 1/frequency and is a function of the thermal conductivity, density, and heat capacity of the material. For an extremely heterogeneous system, heat diffusion could be a complex function. Nevertheless, it is important to investigate the role of heating frequency on the effectiveness of the technique. To achieve this, lock-in thermography was conducted on the AD844 amplifier as a function of lock-in frequencies ranging from 0.125 to 3.0 Hz. Selection of these frequencies is dictated by the constraints in operating the flash lamps. Figure 5 shows the phase maps as a function of frequency, and it is apparent that frequencies from 0.125 to 2.0 Hz show good resolution, yet, noise is present in the phase map taken at 3.0 Hz. The apparent reduction in resolution is most likely attributed to the decrease in the amplitude of the injected thermal signal at higher

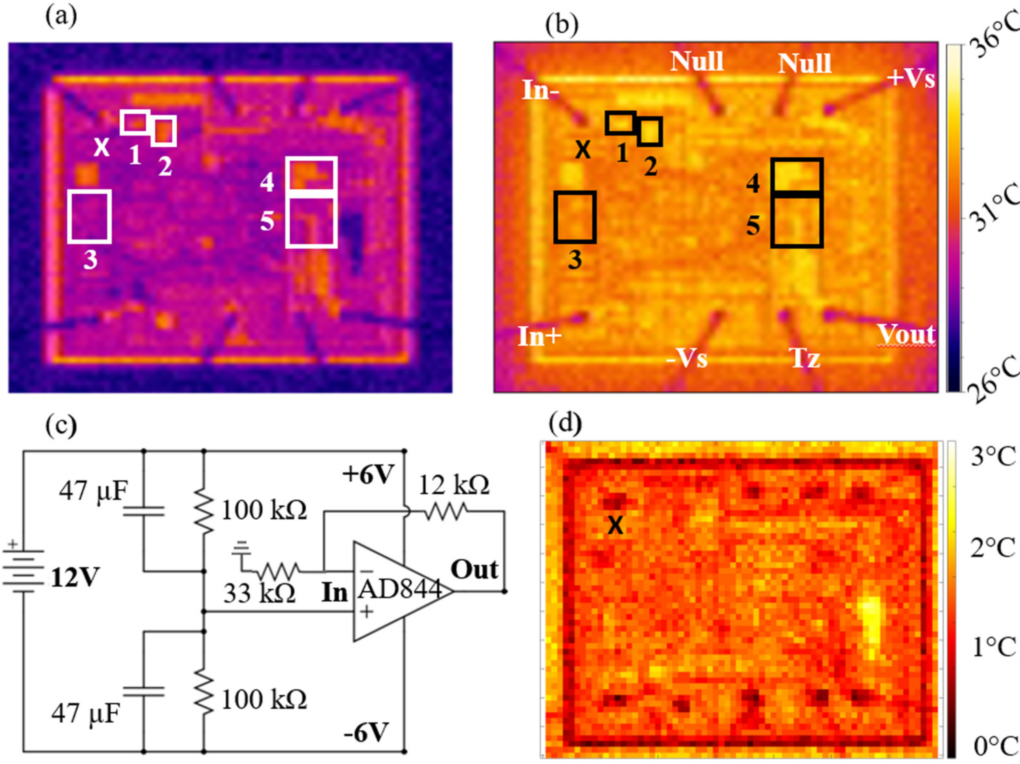

FIG. 4. (a) and (b) Thermal micrographs before and after biasing of the operational amplifier AD844, powered as shown by (c) the circuit schematic, with (d) a map of the change in temperature as a result of biasing.

07 April 2024 11:13:51

Published under an exclusive license by the AVS

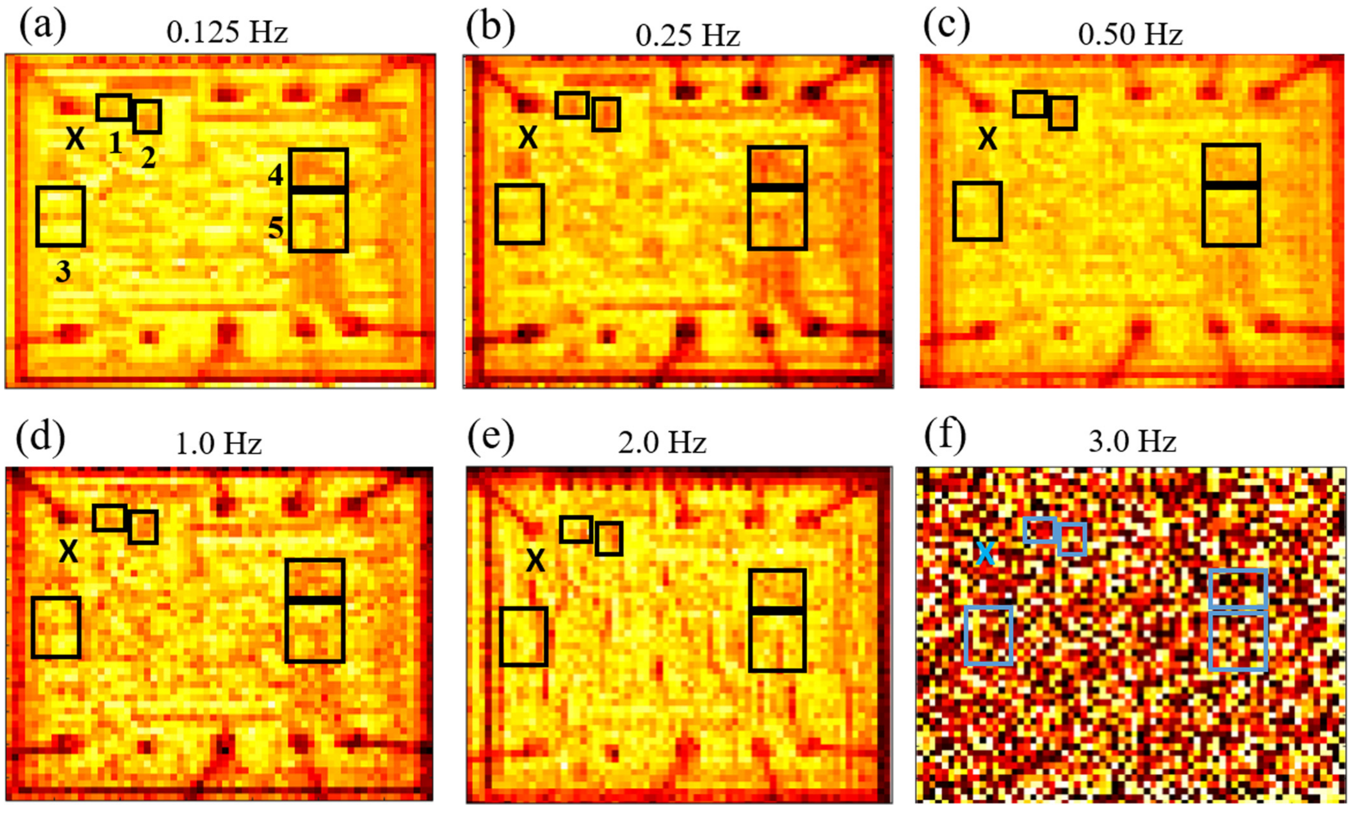

FIG. 5. Phase maps from lock-in thermography analysis of the operational amplifier AD844 for thermal pulse frequencies of (a) 0.125, (b) 0.25, (c) 0.5, (d) 1.0, (e) 2.0, and (f) 3.0 Hz.

07 April 2024 11:13:51

frequencies, which resulted in too low of a signal to resolve frequency information at 3 Hz. The influence of such a low thermal pulse frequency could arise from the complex multilayer, multimaterial structure of the DUT and the infrared sensor. Figure 5, therefore, indicates the need for optimizing the thermal pulse frequency for effective utilization of the technique.

The data from these phase maps and the electrical bias analysis were averaged in the five sensitive, boxed regions as well as the insensitive, "X" region and summarized the data in Table I and visually as a plot in Fig. 6. We see that all of the regions show relatively high phase values, which range from 60% to 80% of the values seen across the entire board. This is rather consistent for all frequencies analyzed. However, there are some interesting results from thermo-electric analysis, with relatively high temperatures at locations 1 and "X," and this may be attributed to the proximity of these regions to the input voltage lead in the upper left, which may be heating these two regions relative to the rest of the board.

As a reminder, we are interested in examining the phase lag from lock-in analysis to identify regions in commercial electronics with high strain. Temperature change due to electrical biasing is used as a metric for identifying areas of electrical activity. Together, we are using the phase and temperature values to predict regions of high sensitivity to radiation. For this analysis, the chips were sectioned to better visualize the phase and temperature data region by region. A metric or composite score that combines the phase and temperature data to extract the region that has the highest probable sensitivity was created using Eq. (2). The phase map that was created with a lock-in frequency of 0.25 Hz was used for its relatively good resolution and contrast,

$$\text{Composite score} = \text{Normalize}\left[\text{Abs}\left(\frac{\varphi - \varphi_{avg}}{\varphi_{max} - \varphi_{min}}\right)\left(\frac{T - T_{min}}{T_{max} - T_{min}}\right)\right]. \tag{2}$$

This composite score accounts for the extreme phase values, which may indicate positive and negative strains and large temperature changes due to biasing. The resulting score is normalized and we have shown the result as a map overlaid on the optical micrograph of the AD844 amplifier in Fig. 6. Electrical and mechanical metrics were multiplied so that regions with generally high phase contrast and electrical activity are highlighted as being particularly sensitive with a high composite score. One metric is not necessarily

Published under an exclusive license by the AVS

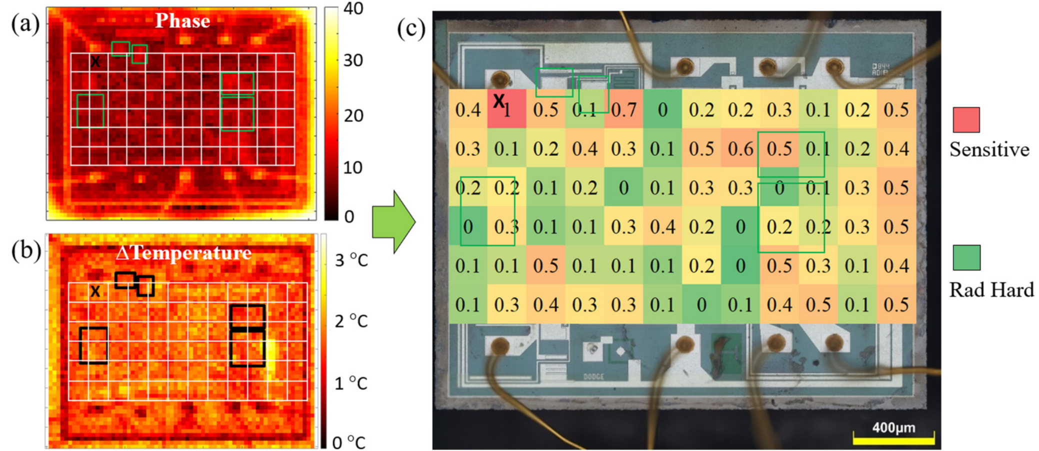

FIG. 6. (a) and (b) Phase and temperature results combined to create a (c) composite score of predictively identifying MVRs overlaid on an optical micrograph of the AD844 amplifier.

more significant than another in terms of its impact on the overall susceptibility because they are both generally necessary to cause damage or an upset. There is not yet a sufficient understanding of these metrics in radiation susceptibility to draw a relative relationship in terms of their impact on device sensitivity. The figure shows a reasonable agreement with literature-defined regions of sensitivity, given that the sensitive regions are not perfectly defined by their outlines and that there is slight spatial variation in the positioning of the sensitive regions from literature with the produced composite score map.

In order to examine the changes in the stress state of the LM124 amplifier due to ionizing radiation exposure, the chip was irradiated at Penn State's Radiation Science and Engineering Center with an isotropic dose of ^{60}Co gamma radiation. The LM124 amplifier received an isotropic dose of 10 krad at 155 krad/h (air) with an overall uncertainty of ±2.4% at a 95% confidence level, which is certified by the National Institute of Standards and Technology using the Fricke dosimetry system under the National Voluntary Laboratory Accreditation Program. Figure 7 shows the pre- and postirradiation changes.

07 April 2024 11:13:51

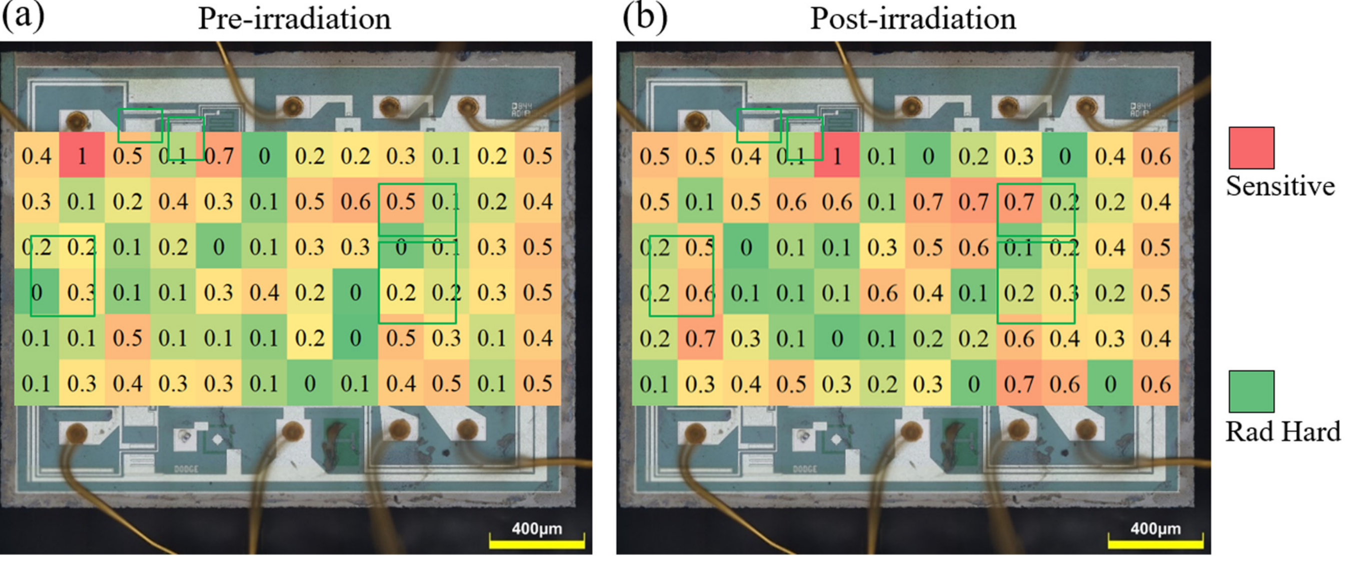

FIG. 7. Composite score of the operational amplifier LM124 (a) before and (b) after ^{60}Co irradiation.

Published under an exclusive license by the AVS

The region of the highest sensitivity, indicated with a "1" in Fig. 7, changes after irradiation, showing that a change in the stress state at the most stressed and sensitive location can be rather significant as a result of irradiation. Across the chip, the composite score shows shifting in values due to irradiation, which indicates the total ionizing dose effects on the LM124 amplifier having an effect on the stress state of the materials that make it up.

IV. SUMMARY AND CONCLUSIONS

This study presents a fast technique for the approximate estimation of radiation-sensitive regions on an entire operational amplifier AD844. The core philosophy behind the proposed technique is that localized, highly strained regions will take less energy (compared to the regions in inter-atomic equilibrium) to ionize. It is important to note that device design, material inhomogeneity, fabrication processing, and operating conditions lead to such localizations even if the global value is negligible. The focus of this study is, therefore, not on the global values, but to highlight the vulnerability caused by these localized strained regions. The implication is that the incoming radiation may not produce any measurable global displacement damage, but the localized strained regions will experience the radiation and will induce more charges to degrade the electronic devices. Another unique aspect of this study is that it does not attempt to precisely locate the localized strained regions, but to accurately detect the "approximate" location over a large area. Thermal phase lag microscopy suits the proposed technique because it allows large areas to be mapped quickly, while approximating the strained regions. A close analogy to this detection philosophy is as follows: an object that is smaller than the wavelength of white light cannot be resolved with white light microscopy, but it still can be detected. Therefore, the contribution of the proposed technique is a very fast, accurate detection of radiation-vulnerable regions with approximate spatial mapping. The technique, therefore, can be impactful for large specimens, such as a system on a chip, for which precise localization mapping may take an infeasible amount of time.

Localized mechanical stress and electrical field are used to predictively identify the most vulnerable regions in microelectronics to ionizing radiation. The AD844 amplifier has been observed to have five sensitive regions from using the validated pulsed-laser single event transient technique in the literature. A composite score was constructed from the combination of pulsed thermal phase analysis via lock-in thermography and electrical biasing analysis to identify regions as vulnerable to radiation-induced upsets. The results from this study showed consistency with the literature results, but it must be noted that the method for electrical field analysis is nonideal, and as a result, the composite map does not show a perfect prediction. Yet, the prediction can provide additional locations of interest for further evaluation using pulsed-laser techniques. As a result, this study can significantly reduce the time required for the analysis of electronics, especially for larger and more complex devices, for which traditional analysis would take —two to three orders of magnitude more time to complete. At the same time, the strength of the technique, namely, characterization speed, could also be the weakness. The indirect nature of identifying mechanical and electrical hotspots requires more studies for validation. The spatial resolution could also be improved by higher magnification infrared microscopy.

ACKNOWLEDGMENTS

This work was funded by the Department of Defense, Defense Threat Reduction Agency (DTRA) as part of the Interaction of Ionizing Radiation with Matter University Research Alliance (IIRM-URA) under Contract No. HDTRA1-20-2-0002. The content of the information does not necessarily reflect the position or the policy of the federal government, and no official endorsement should be inferred. A.H. also acknowledges support from the U.S. National Science Foundation (ECCS No. 2015795).

AUTHOR DECLARATIONS

Conflict of Interest

The authors have no conflicts to disclose.

Author Contributions

Sergei P. Stepanoff: Data curation (equal); Formal analysis (equal); Investigation (equal); Methodology (equal); Validation (equal); Visualization (equal); Writing – original draft (equal). **Aman Haque:** Conceptualization (equal); Formal analysis (equal); Funding acquisition (equal); Investigation (equal); Methodology (equal); Project administration (equal); Resources (equal); Supervision (equal); Validation (equal); Writing – review & editing (equal). **Fan Ren:** Funding acquisition (equal); Project administration (equal); Resources (equal); Validation (equal); Writing – review & editing (equal). **Stephen Pearton:** Conceptualization (equal); Funding acquisition (equal); Methodology (equal); Project administration (equal); Writing – review & editing (equal). **Douglas E. Wolfe:** Conceptualization (equal); Funding acquisition (equal); Investigation (equal); Project administration (equal); Resources (equal); Supervision (equal); Writing – review & editing (equal).

DATA AVAILABILITY

The data that support the findings of this study are available from the corresponding author upon reasonable request.

REFERENCES

[1]S. Gerardin and M. Bagatin, *Ionizing Radiation Effects in Electronics* (CRC, Boca Raton, 2016).
[2]B. Beeler, M. Asta, P. Hosemann, and N. Grønbech-Jensen, J. Nucl. Mater. **459**, 159 (2015).
[3]G. F. Knoll, *Radiation Detection and Measurement*, 4th ed. (Wiley, Hoboken, NJ, 2010).
[4]R. N. S. Raphael *et al.*, in *Proceedings of the 3rd Brazilian Technology Symposium* (Springer Nature, Switzerland, 2019), pp. 223–238.
[5]M. Bagatin and S. Gerardin, *Ionizing Radiation Effects in Electronics from Memories to Imagers* (CRC, Boca Raton, 2018).
[6]C. F. Pien, Am. J. Appl. Sci. **7**, 807 (2010).
[7]H. J. Barnaby, M. l. Mclain, and I. S. Esqueda, Nucl. Instrum. Methods Phys. Res. Sec. B: Beam Interact. Mater. Atoms, **261**, 1142–1145 (2007).
[8]C. Gu, R. Chen, G. Belev, S. Shi, H. Tian, I. Nofal, and L. Chen, Materials **12**, 3411 (2019).
[9]Y.-T. Yu, J.-W. Han, G.-Q. Feng, M.-H. Cai, and R. Chen, IEEE Trans. Nucl. Sci. **62**, 565 (2015).

07 April 2024 11:13:51

Published under an exclusive license by the AVS

[10]F. Miller *et al.*, "Laser Mapping of SRAM Sensitive Cells: A Way to Obtain Input Parameters for DASIE Calculation Code," in *IEEE Transactions on Nuclear Science* (IEEE, 2006), Vol. 53, No. 4, pp. 1863–1870.
[11]A. M. Chugg, A. J. Burnell, M. J. Moutrie, R. Jones, and R. Harboe-Sorensen, IEEE Trans. Nucl. Sci. **54**, 2106 (2007).
[12]V. Pouget, H. Lapuyade, D. Lewis, Y. Deval, P. Fouillat, and L. Sarger, "SPICE modeling of the transient response of irradiated MOSFETs," in *IEEE Transactions on Nuclear Science* (IEEE, 2000), Vol. 47, No. 3, pp. 508–513.
[13]D. McMorrow, W. T. Lotshaw, J. S. Melinger, S. Buchner, Y. Boulghassoul, L. W. Massengill, and R. L. Pease, IEEE Trans. Nucl. Sci. **50**, 2199 (2003).
[14]F. R. Palomo, J. M. Mogollon, J. Napoles, and M. A. Aguirre, "Mixed-Mode Simulation of Bit-Flip With Pulsed Laser," in *IEEE Transactions on Nuclear Science* (IEEE, 2010), Vol. 57, No. 4, pp. 1884–1891.
[15]P. E. Dodd *et al.*, IEEE Trans. Nucl. Sci. **54**, 2303 (2007).
[16]D. Aktah and I. Frank, J. Am. Chem. Soc. **124**, 3402 (2002).
[17]S. Garcia-Manyes and A. E. M. Beedle, Nat. Rev. Chem. **1**, 11 (2017).
[18]M. C. Sequeira, F. Djurabekova, K. Nordlund, J.-G. Mattei, I. Monnet, C. Grygiel, E. Alves, and K. Lorenz, Small **18**, 2102235 (2022).
[19]S. P. Stepanoff, M. A. J. Rasel, A. Haque, D. E. Wolfe, F. Ren, and S. J. Pearton, ECS J. Solid State Sci. Technol. **11**, 085008 (2022).
[20]Y. Sun, S. E. Thompson, and T. Nishida, *Strain Effect in Semiconductors* (Springer US, Boston, MA, 2010).
[21]B. Ghyselen *et al.*, Solid State Electron. **48**, 1285 (2004).
[22]M. A. J. Rasel, S. Stepanoff, A. Haque, D. E. Wolfe, F. Ren, and S. Pearton, Phys. Status Solidi RRL **16**, 2200171 (2022).
[23]M. Gaillardin, S. Girard, Y. Ouerdane, A. Boukenter, F. Andrieu, C. Tabone, and O. Faynot, J. Non-Cryst. Solids **357**, 1989 (2011).
[24]M. Gaillardin *et al.*, IEEE Trans. Nucl. Sci. **61**, 1628 (2014).
[25]C. Gu, D. Hiemstra, V. Kirischian, and L. Chen, "Single Event Transients Detection in AD844 Operational Amplifier by Utilizing Ultra-fast Pulsed Laser System," in *2020 IEEE Radiation Effects Data Workshop (in conjunction with 2020 NSREC)*, Santa Fe, NM (IEEE, 2020), pp. 1–6.
[26]C. Gu, "Study of single event effects by ultra-fast pulsed laser system," Doctoral thesis (University of Saskatchewan, 2020).
[27]O. Breitenstein, W. Warta, and M. C. Schubert, *Lock-in Thermography Basics and Use for Evaluating Electronic Devices and Materials*, 3rd ed. (Springer, Berlin, 2018), p. 10.

07 April 2024 11:13:51

Published under an exclusive license by the AVS